

鳥取大学研究成果リポジトリ  
Tottori University research result repository

タイトル Title	Potassiation and Depotassiation Properties of Sn4P3 Electrode in an Ionic-Liquid Electrolyte
著者 Author(s)	Domi, Yasuhiro; Usui, Hiroyuki; Nakabayashi, Eisuke; Yamamoto, Takayuki; Nohira, Toshiyuki; Sakaguchi, Hiroki
掲載誌・巻号・ページ Citation	ELECTROCHEMISTRY , 87 (6) : 333 - 335
刊行日 Issue Date	2019
資源タイプ Resource Type	学術雑誌論文 / Journal Article
版区分 Resource Version	著者版 / Author
権利 Rights	(C) 2019 The Electrochemical Society of Japan
DOI	<a href="https://doi.org/10.5796/electrochemistry.19-00052">10.5796/electrochemistry.19-00052</a>
URL	<a href="https://repository.lib.tottori-u.ac.jp/9004">https://repository.lib.tottori-u.ac.jp/9004</a>

Potassiation and Depotassiation Properties of Sn<sub>4</sub>P<sub>3</sub> Electrode in an Ionic-Liquid  
Electrolyte

Yasuhiro Domi,<sup>1,3</sup> Hiroyuki Usui,<sup>1,3</sup> Eisuke Nakabayashi,<sup>2,3</sup> Takayuki Yamamoto,<sup>4</sup>

Toshiyuki Nohira,<sup>4</sup> and Hiroki Sakaguchi<sup>1,3,\*</sup>

<sup>1</sup>Department of Chemistry and Biotechnology, Graduate School of Engineering, Tottori  
University, Minami 4–101, Koyama–cho, Tottori 680–8552, Japan

<sup>2</sup>Course of Chemistry and Biotechnology, Department of Engineering, Graduate School  
of Sustainability Science, Tottori University, Minami 4–101, Koyama–cho, Tottori 680–  
8552, Japan

<sup>3</sup>Center for Research on Green Sustainable Chemistry, Tottori University, Minami 4–101,  
Koyama–cho, Tottori 680–8552, Japan

<sup>4</sup>Institute of Advanced Energy, Kyoto University, Uji 611–0011, Japan

\*Corresponding Author

Hiroki Sakaguchi

E-mail: sakaguch@tottori-u.ac.jp

## **Abstract**

K-ion battery is a potential candidate as a next-generation battery with a high energy density, long cycle life, and high safety. To commercialize the battery, the improvement of safety is absolutely essential. We apply a nonflammable ionic-liquid electrolyte to a  $\text{Sn}_4\text{P}_3$  electrode as negative-electrode for K-ion battery. The electrode achieves the excellent cycling performance with a discharge capacity of  $365 \text{ mA h g}^{-1}$  over 100 cycles in the ionic-liquid electrolyte. Rate capability in the ionic-liquid electrolyte is almost the same as that in the organic-liquid electrolyte.

*Keyword; K-ion battery,  $\text{Sn}_4\text{P}_3$ , negative electrode, ionic-liquid electrolyte*

## 1. Introduction

Toward building a sustainable society, there is an increased demand for rechargeable alkali-metal-ion batteries with a high energy density, long cycle life, and adequate safety. Li-ion battery (LIB) has been commercially utilized due to the advantage of the lowest standard electrode potential among alkali metals and the lightest atomic weight. However, the abundance of lithium in the Earth's crust is only 20 ppm, and lithium metal reserve is unevenly distributed in South America.<sup>1</sup> Thus, Na-ion battery (NIB) attracts attention because of the second lightest atomic weight among alkali metals, abundant resources, and nontoxicity. Many researchers have spent considerable effort on the development of active materials for NIB.<sup>2,3</sup> We have also synthesized various active materials for negative electrodes in NIB.<sup>4,5</sup> Among them, Sn<sub>4</sub>P<sub>3</sub> electrode has exhibited superior sodiation/desodiation properties in a pyrrolidinium-based ionic-liquid electrolyte.<sup>4</sup>

It was reported that a Sn<sub>4</sub>P<sub>3</sub>/C electrode showed a reversible capacity of 385 mA h g<sup>-1</sup> at 50 mA g<sup>-1</sup> in an organic-liquid electrolyte of 0.8 mol dm<sup>-3</sup> (M) KPF<sub>6</sub> dissolved in ethylene carbonate (EC) + diethyl carbonate (DEC) and maintained the capacity up to 40 cycles.<sup>6</sup> The theoretical capacity of the Sn<sub>4</sub>P<sub>3</sub> electrode is 802 mA h g<sup>-1</sup> when K<sub>3</sub>P and K<sub>2</sub>Sn phases are formed in the charge process.<sup>7,8</sup> Assuming that a KSn phase is formed

instead of  $K_2Sn$ , the theoretical capacity is estimated to be  $614 \text{ mA h g}^{-1}$ . K-ion battery (KIB) is attractive as a next-generation rechargeable battery because the standard electrode potential of potassium is  $-2.94 \text{ V}$  vs. standard hydrogen electrode (SHE) in water at  $298 \text{ K}$ , close to lithium ( $-3.04 \text{ V}$  vs. SHE). Interestingly, the standard electrode potential of potassium is lower than that of lithium in some organic-liquid electrolytes including propylene carbonate and EC+DEC.<sup>9,10</sup> In molten alkali bis(fluoromethanesulfonyl)amide at intermediate temperature, the similar tendency is indicated.<sup>11</sup> Therefore, KIB is worth investigating as a high energy density rechargeable battery.

Ignition risk increases with an increase in the atomic number of alkali metals; potassium intensely reacts with moisture. The improvement of KIB safety is absolutely essential for its commercialization. As a safe electrolyte, ionic liquids are potential candidates as alternatives to flammable carbonate-based organic-liquid electrolytes because of their superior physicochemical properties, such as nonflammability and wide electrochemical windows.<sup>12</sup> We have demonstrated that the cells with Si-based electrodes for LIB delivered not only high safety but also excellent electrochemical performance in ionic-liquid electrolytes compared to that in usual organic-liquid electrolytes.<sup>13,14</sup> This study explored the applicability of an ionic-liquid electrolyte to the  $Sn_4P_3$  negative

electrode for KIB to improve the electrochemical performance and safety of the electrode.

## 2. Experimental

$\text{Sn}_4\text{P}_3$  powder was synthesized by a mechanical alloying (MA) method. Synthesis procedure and characterization were described in our previous report.<sup>4</sup> A  $\text{Sn}_4\text{P}_3$  electrode was fabricated by a slurry coating method. The synthesized active material powder of  $\text{Sn}_4\text{P}_3$  was mixed with a conductive agent of acetylene black (AB) and a binder of carboxymethyl cellulose (CMC) and styrene-butadiene rubber (SBR). The weight ratio of  $\text{Sn}_4\text{P}_3$ /AB/CMC/SBR was 70/15/10/5 wt.%. Deionized water was used as a dispersing agent. The prepared slurry was pasted on a Cu current collector and was dried to form active material layer (120°C). The mass loading and film thickness of active material layer were about  $0.89 \text{ mg cm}^{-2}$  and  $15 \text{ }\mu\text{m}$ , respectively. 2032-type coin cell was assembled in an Ar-filled glove box with a dew point below  $-90^\circ\text{C}$  and an oxygen content less than 1 ppm. The  $\text{Sn}_4\text{P}_3$  slurry electrode, potassium metal sheet, and a glass fiber filter (Whatman GF/A) was used as the working electrode, the counter electrode, and the separator, respectively. We used an ionic-liquid electrolyte comprised of potassium bis(fluorosulfonyl)amide (KFSA) dissolved in *N*-methyl-*N*-propylpyrrolidinium bis(fluorosulfonyl)amide (Py13-FSA or  $[\text{C}_3\text{C}_1\text{pyrr}][\text{FSA}]$ ). The molar ratio of KFSA to

Py13-FSA was 20:80 mol% (molar concentration is  $0.9744 \text{ mol dm}^{-3}$  at 303 K). Physicochemical and electrochemical properties of the ionic-liquid electrolyte have been previously reported in detail.<sup>15</sup> The cell was galvanostatically charged and discharged between 0.005 and 2.000 V vs  $\text{K}^+/\text{K}$  at 303 K. The current density was set at  $50 \text{ mA g}(\text{Sn}_4\text{P}_3)^{-1}$ . The rate capability was also estimated at current rates from 50 to  $1000 \text{ mA g}(\text{Sn}_4\text{P}_3)^{-1}$ .

### 3. Results and discussion

Figure 1(a) shows the charge–discharge curve of a  $\text{Sn}_4\text{P}_3$  electrode in an ionic-liquid electrolyte of potassium bis(fluorosulfonyl)amide (KFSA) dissolved in *N*-methyl-*N*-propylpyrrolidinium bis(fluorosulfonyl)amide (Py13-FSA or  $[\text{C}_3\text{C}_1\text{pyrr}][\text{FSA}]$ ). The molar ratio of KFSA to Py13-FSA was 20:80 mol%. The electrode exhibits a potential slope between 0.7 and 0.3 V (vs.  $\text{K}^+/\text{K}$ ) and a potential plateau at around 0.2 V on the first charge curve (Figure 1(b)). The reductive decomposition of electrolyte occurs above 0.3 V, which results in surface film formation. At 0.2 V, the potassiation reaction of  $\text{Sn}_4\text{P}_3$  should occur. On the first discharge curve, a definitive potential plateau is not confirmed; the  $\text{Sn}_4\text{P}_3$  electrode shows a potential shoulder from 0.2 to 1.2 V. Additionally, a potential slope appears between 0.6 and 0 V in the second charge process instead of the potential

plateau at around 0.2 V. Zhang et al. proposed a reversible reaction of Sn<sub>4</sub>P<sub>3</sub> during potassiation/depotassiation in an organic-liquid electrolyte based on X-ray diffraction.<sup>6,16</sup> However, this mechanism differs from sodiation/desodiation mechanism of Sn<sub>4</sub>P<sub>3</sub> by a phase separation in the ionic-liquid electrolyte.<sup>4</sup> We try to clarify the reaction mechanism of Sn<sub>4</sub>P<sub>3</sub> with potassium in the electrolyte.

Figure 2 shows cycling performance of the Sn<sub>4</sub>P<sub>3</sub> electrode in the ionic-liquid electrolyte. The electrode exhibits initial reversible capacity of ca. 400 mA h g<sup>-1</sup>, which is more than 1.5 times higher than that of a graphite-based electrode.<sup>10</sup> Additionally, the Sn<sub>4</sub>P<sub>3</sub> electrode maintains a discharge capacity of 365 mA h g<sup>-1</sup> over 100 cycles; no degradation of the cycling performance occurs up to the 100th cycle in the ionic-liquid electrolyte of KFSA/Py13-FSA (20/80 mol%). While the initial capacity of the Sn<sub>4</sub>P<sub>3</sub> electrode in an organic-liquid electrolyte of 0.8 M KPF<sub>6</sub>/EC+DEC was almost the same as that in the ionic-liquid electrolyte, the capacity faded at around the 40th cycle in the organic-liquid electrolyte.<sup>6</sup>

The difference in cycling performance should be attributed to properties of surface film formed on the Sn<sub>4</sub>P<sub>3</sub> electrode in each electrolyte. In the organic-liquid electrolyte, a surface film with uneven thicknesses forms through reductive decomposition of the electrolyte. Concentrative potassiation/depotassiation reactions

occur on the thinner parts of the film because the thicker parts prevent the  $K^+$  storage, as we have demonstrated for Si negative-electrode in LIB.<sup>13</sup> Hence, local change in the volume of  $Sn_4P_3$  occurs, which leads to disintegration of the active material layer and rapid capacity fading. By contrast, in the ionic-liquid electrolyte, a uniform and thin surface film should be formed and  $K^+$  is homogeneously stored on the entire electrode surface, preventing the occurrence of local stress. Thus, severe disintegration of  $Sn_4P_3$  electrode is suppressed, which provides excellent performance of the  $Sn_4P_3$  electrode. In addition, KFSA salt should support good cyclability for the electrode.<sup>16</sup> While the first Coulombic efficiency is only 66.7%, the second efficiency reaches 98.2%. Higher efficiency of 99.8% is also confirmed at the 20th cycle. High Coulombic efficiency after the second cycle is characteristic of the combination of  $Sn_4P_3$  electrode and Py13-FSA ionic-liquid electrolyte.<sup>4</sup>

Figure 3 gives rate capability of the  $Sn_4P_3$  electrode in the ionic-liquid electrolyte. The electrode exhibits an initial discharge capacity of ca. 400 mA h  $g^{-1}$  at a current density of 50 mA  $g^{-1}$ . The reversible capacity gradually decreases with an increase in the current density and the capacity of 100 mA h  $g^{-1}$  is confirmed at 1000 mA  $g^{-1}$  between 21st and 25th cycles, which is approximately half of the capacity in inorganic-liquid electrolyte at the same current density.<sup>6</sup> However, with a prolonged rate capability test, the capacity of

the Sn<sub>4</sub>P<sub>3</sub> electrode reaches 200 mA h g<sup>-1</sup> at 1000 mA g<sup>-1</sup> between 46th and 50th cycles, which is comparable to the performance in the organic-liquid electrolyte.<sup>6</sup> There are some possibilities of these phenomena: a surface film growth with better properties by repeated charge-discharge cycling, activation process of active material of Sn<sub>4</sub>P<sub>3</sub>, and so on. We are now trying to clarify these possibilities. Additionally, the discharge capacity recovers at the initial current density of 50 mA g<sup>-1</sup>; thus, no electrode disintegration occurs. Consequently, the rate performance of Sn<sub>4</sub>P<sub>3</sub> electrode is almost the same in both ionic- and organic-liquid electrolytes.

#### **4. Conclusions**

A Sn<sub>4</sub>P<sub>3</sub> electrode exhibited a superior cycling performance with reversible capacity of 365 mA h g<sup>-1</sup> over 100cycles in a certain ionic-liquid electrolyte of KFSA/Py13-FSA (20/80 mol%). To commercialize KIB, the improvement of safety is very important. The electrode achieved not only high safety but also excellent cycling and rate performances for KIB in the ionic-liquid electrolyte compared to that in the organic-liquid electrolyte.

#### **Acknowledgments**

This study was partially supported by Joint Usage/Research Program on Zero-Emission Energy Research, Institute of Advanced Energy, Kyoto University (ZE30A-06, ZE31A-08), and Japan Society for the Promotion of Science (JSPS) KAKENHI (Grant Numbers 19K05649, 19H02817, 17H03128).

## References

1. N. Yabuuchi, K. Kubota, M. Dahbi, S. and Komaba, *Chem. Rev.*, **114**, 11636 (2014).
2. K. Gotoh, T. Ishikawa, S. Shimadzu, N. Yabuuchi, S. Komaba, K. Takeda, A. Goto, K. Deguchi, S. Ohki K. Hashi, T. Shimizu, and H. Ishida, *J. Power Sources*, **225**, 137 (2013).
3. S. Kaushik, K. Matsumoto, Y. Sato, and R. Hagiwara, *Electrochem. Commun.*, **102**, 46 (2019).
4. H. Usui, Y. Domi, K. Fujiwara, M. Shimizu, T. Yamamoto, T. Nohira, R. Hagiwara, and H. Sakaguchi, *ACS Energy Lett.*, **2**, 1139 (2017).
5. H. Usui, Y. Domi, R. Yamagami, K. Fujiwara, H. Nishida, and H. Sakaguchi, *ACS Appl. Energy Mater.* **1**, 306 (2018).
6. W. Zhang, J. Mao, S. Li, Z. Chen, and Z. Guo, *J. Am. Chem. Soc.*, **139**, 3316 (2017).
7. J. Sangster, and C. W. Bale, *J. Phase Equilib.*, **19**, 67 (1998).
8. J. Sangster, *J. Phase Equilib. Diff.*, **31**, 68 (2010).
9. Y. Marcus, *Pure & Appl. Chem.*, **57**, 1129 (1985).
10. S. Komaba, T. Hasegawa, M. Dahbi, K. Kubota, *Electrochem. Commun.*, **60**, 172 (2015).
11. A. Watarai, K. Kubota, M. Yamagata, T. Goto, T. Nohira, R. Hagiwara, K. Ui, and N. Kumagai, *J. Power Sources*, **183**, 724 (2008).

12. P. Hapiot, and C. Lagrost, *Chem. Rev.*, **108**, 2238 (2008).
13. Y. Domi, H. Usui, K. Yamaguchi, S. Yodoya, and H. Sakaguchi, *ACS Appl. Mater. Interfaces*, **11**, 2950 (2019).
14. K. Yamaguchi, Y. Domi, H. Usui, M. Shimizu, S. Morishita, S. Yodoya, T. Sakata, and H. Sakaguchi, *J. Electrochem. Soc.* **166**, A268 (2019).
15. T. Yamamoto, K. Matsumoto, R. Hagiwara, and T. Nohira, *J. Phys. Chem. C* **121**, 18450 (2017).
16. W. Zhang, W. K. Pang, V. Sencadas, and Z. Guo, *Joule.*, **2**, 1534 (2018).

Figure captions

Figure 1 (a) Charge-discharge curve of a  $\text{Sn}_4\text{P}_3$  electrode in KFSA/Py13-FSA (20/80 mol%) and (b) differential capacity plot of the first cycle.

Figure 2 Cycling performance of a  $\text{Sn}_4\text{P}_3$  electrode in KFSA/Py13-FSA (20/80 mol%).

Figure 3 Rate performance of a  $\text{Sn}_4\text{P}_3$  electrode in KFSA/Py13-FSA (20/80 mol%).

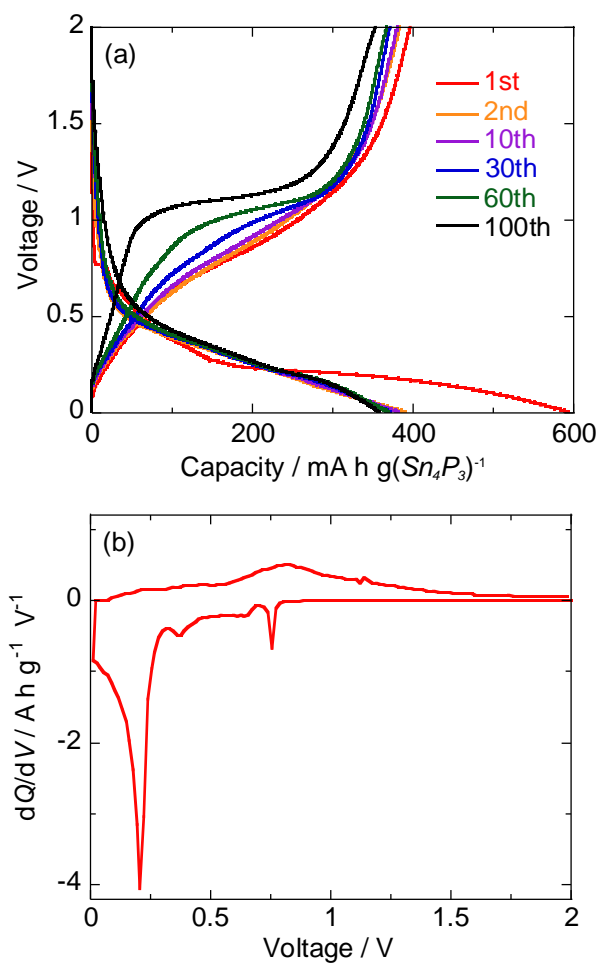


Figure 1

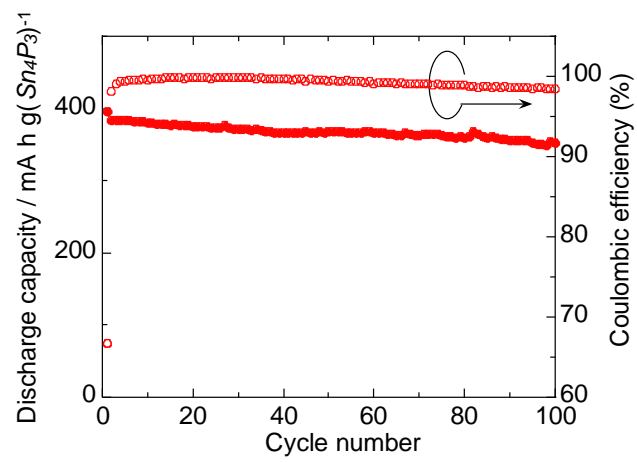


Figure 2

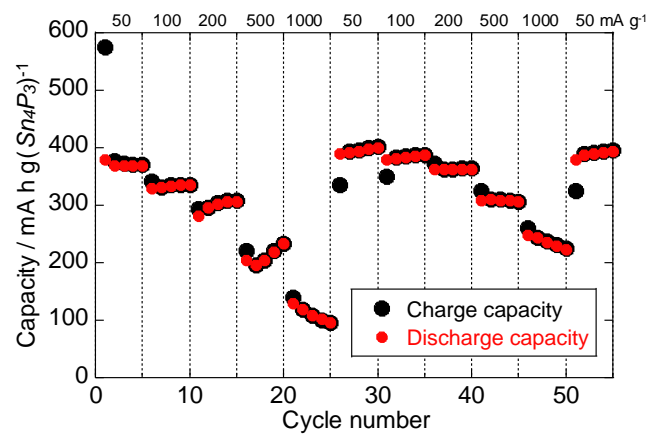


Figure 3